Journal of Computer-Aided Molecular Design, 10 (1996) 89–99
ESCOM

J-CAMD 333

Conformational and receptor-binding properties of the insect neuropeptide proctolin and its analogues

Barbara Odell[a,*], Stephen J. Hammond[a,**], Richard Osborne[b] and Michael W. Goosey[a,***]

[a]*Shell Research Ltd, Sittingbourne Research Centre, Sittingbourne, Kent ME9 8AG, U.K.*
[b]*Department of Biology, University of the West of England, Frenchay Campus, Bristol BS16 1QY, U.K.*

Received 17 July 1995
Accepted 22 December 1995

Keywords: Conformation; Molecular dynamics; NMR

Summary

Proctolin (Arg-Tyr-Leu-Pro-Thr) was the first insect neuropeptide to be chemically characterised. It plays an essential role in insect neurophysiology and is involved in muscular contraction and neuromodulation. Elements of secondary structure in solution have been studied by comparing data obtained from NMR and molecular dynamics simulations. Different secondary structural requirements are associated with agonist and antagonist activities. A favoured conformation of proctolin has an inverse γ-turn, comprising an intramolecular hydrogen bond near the C-terminal end between Thr NH and Leu CO. Antagonists have a more compact structure resembling a 'paperclip' loop, containing an intramolecular hydrogen bond between Tyr NH and Pro CO, possibly stabilised by a salt bridge between the N- and C-terminal groups. A cyclic analogue retains antagonist activity and resembles a β-bulge loop, also comprising intramolecular hydrogen bonds between Tyr NH and Pro CO and Thr CO. These models may offer feasible starting points for designing novel compounds with proctolinergic activity.

Introduction

The pentapeptide proctolin was first isolated by Brown and Starratt as the active component from foregut extracts of the cockroach *Periplaneta americana*, in which it causes contraction of the longitudinal muscles [1]. In addition, proctolin has also been shown to stimulate cockroach heartbeat [2], the locust oviduct [3], hindgut [4] and foregut [5]. Proctolin is ubiquitous among insects and arthropods and is found in nervous tissue, digestive tract, heart as well as in skeletal and smooth muscles [6], suggesting it may play an important role as an excitory modulator of visceral muscle.

Only limited structure–activity data for receptor binding of proctolin and peptide analogues exist. A recent study of proctolin binding on locust oviduct membranes [7] indicated that binding was saturated, specific and reversible, and that only one peptide analogue was an effective competitor. It would appear that any reduction in peptide-chain length causes a loss of agonist activity [1,5]. The quantitative relationship between peptide conformation, receptor binding and biological activity is poorly understood and requires a detailed knowledge of the peptide/receptor complex as provided by X-ray crystallography or NMR spectroscopy [8].

Since proctolin receptors have not been isolated, we have investigated conformational properties of proctolin and analogues in the unbound state to provide some information on the relationship between proctolin conformation and receptor binding. NMR spectroscopy has been used to probe the conformations of proctolin and four analogues in various solvents, and these properties have been related to receptor-binding activity.

Materials and Methods

Peptides

Proctolin acetate ($CH_3CO_2^-NH_3^+$-Arg-Tyr-Leu-Pro-Thr)

*Present address: Albright and Wilson Ltd., International Technical Centre, P.O. Box 80, Trinity Street, Oldbury, Warley, West Midlands B69 4LN2, U.K.
**To whom correspondence should be addressed at: Shell Research and Technology Centre, Thornton, P.O. Box 1, Chester, Cheshire CH1 3SH, U.K.
***Present address: Shell Research and Technology Centre, Thornton, P.O. Box 1, Chester, Cheshire CH1 3SH, U.K.

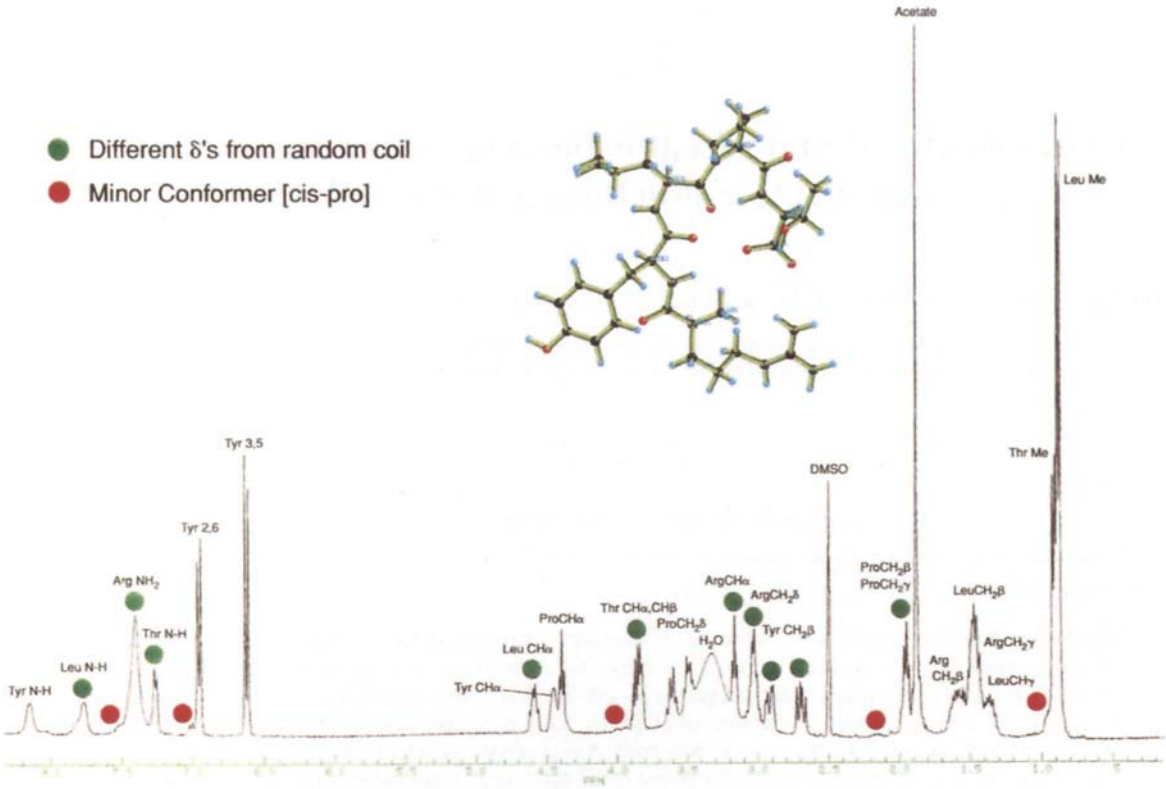

Fig. 1. 360 MHz ^{1}H NMR spectrum of proctolin in DMSO-d_6 recorded at 303 K.

was purchased from Sigma Chemical Company (Poole, U.K.). *N*-Methyl-Leu-proctolin and *N*-methyl-Tyr-proctolin were purchased from Peninsula Laboratories (St. Helens, U.K.) and C^{α}-methyl-Tyr-proctolin and cyclo-proctolin from Nova Biochemicals (Nottingham, U.K.). The purity of the peptides was verified by reverse-phase HPLC, FAB mass spectrometry and ^{1}H NMR spectroscopy.

Functional bio-assay

Isolated foreguts of adult locusts (*Schistocerca gregaria*) were incubated in a Clarke Insect Ringer, contained in organ baths with a volume of 5 ml (NaCl, 113.7 mM; KCl, 1.9 mM; $CaCl_2$, 1.1 mM; $NaHCO_3$, 0.12 mM; Na_2HPO_4, 0.07 mM; pH 6.8) at room temperature for 20 min, prior to testing the effects of proctolin and a range of analogues. The testing was performed using a 6 min dose–response cycle containing two washes, and a 2 min recording period for monitoring the effects of the compounds. The responses of the tissues were recorded via isotonic transducers; the output was fed to an ink-writing oscillograph via an FC117 coupler. For isotonic recording of the isolated foregut, ligatures were placed at the oesophageal and proventricular regions. The proventricular ligature was attached to a glass rod in a vertical organ bath, the contents of which were aerated. A constant tension of 100 mg was placed on the tissue. Proctolin effects were tested on all tissues, prior to testing the ana-

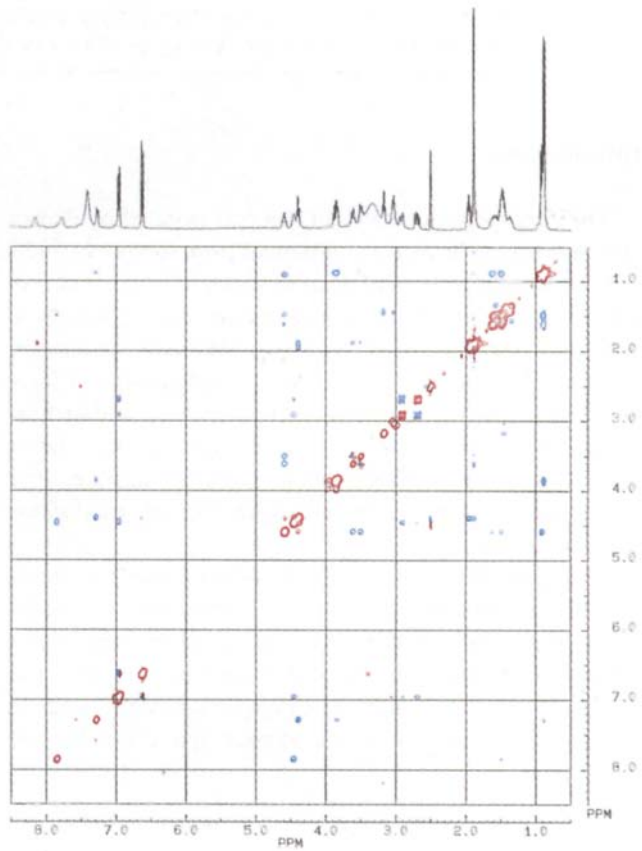

Fig. 2. ROESY spectrum of proctolin in DMSO-d_6 (performed on an AM-360 Bruker NMR instrument) at 303 K.

TABLE 1
NMR AMIDE PROTON TEMPERATURE COEFFICIENTS FOR PROCTOLIN IN DMSO-d_6, CD_3OH AND H_2O/D_2O

Solvent	$\Delta\delta/T$ ($\times 10^{-3}$; ppm/°C)[a]				Dielectric constant at 20 °C
	Arg NH_2	Tyr NH	Leu NH	Thr NH	
DMSO-d_6	5.06	4.67	8.67	1.20	45
CD_3OH	[b]	[b]	10.70	2.70	33
H_2O/D_2O[c]	[b]	[b]	–	8.50	80.4

Temperature range: 30–60 °C at 5° intervals.
[a] Coefficient of change in chemical shift with temperature.
[b] Exchangeable NH.
[c] 10% D_2O.

logues for agonist or antagonist effects. Dose–response curves were constructed for proctolin and its analogues. The tissues were incubated with the potential antagonists for 20 min prior to retesting the effects of proctolin on the tissues.

NMR spectroscopy

Deuterated solvents, i.e. D_2O, DMSO-d_6 and CD_3OH, were purchased from Fluorochem Ltd. (Old Glossop, U.K.). ^1H NMR spectra were recorded on 500-µl samples at 15.4 mM final concentration. High-resolution proton spectra were obtained on a Bruker AM-360 spectrometer operating at 360 MHz with temperature control at 30 ± 1 °C. For 1D spectra, typical spectrum parameters consisted of 32–128 transients collected over a spectral width of 4000 or 5000 Hz with 16K time-domain points, using a relaxation delay of 2.0 s.

Temperature dependences of NH chemical shifts were measured from spectra collected at temperatures ranging from 20 to 60 °C. ^1H assignments were made employing the standard Bruker DISNMR microprograms for homonuclear decoupling and DQF-COSY, using 2K data points digitised in t_2 with 512 FIDs consisting of 32 transients collected in t_1. Zero-filling in t_1 and t_2 resulted in a final 2K-by-1K transformed matrix with digital resolutions of 2.2 Hz/point in F2 and 4.3 Hz/point in F1. A 60° phase-shifted sine bell was applied in both directions before Fourier transformation.

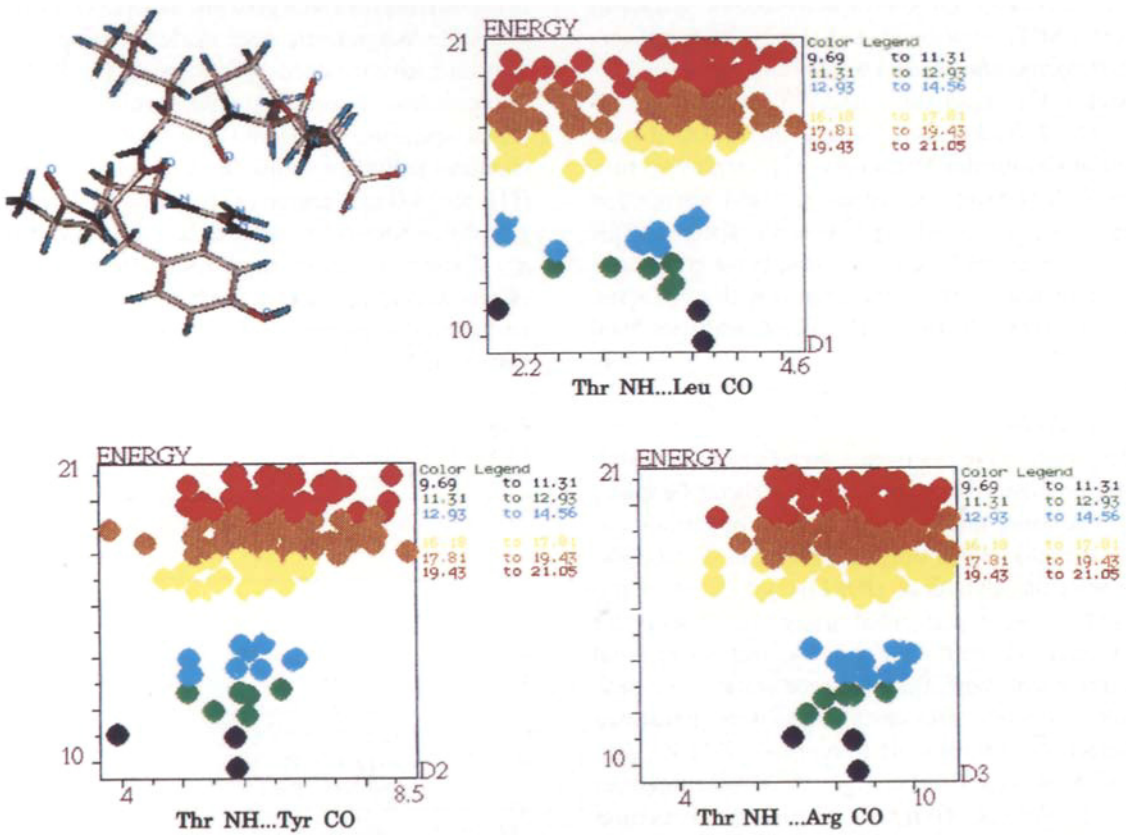

Fig. 3. NH···CO distances obtained from a typical molecular dynamics simulation of proctolin without any constraints, using a dielectric constant of 45 to represent DMSO and the TABLE option in SYBYL.

TABLE 2
CHEMICAL SHIFTS OF PROCTOLIN CARBONYL RESONANCES IN DMSO-d_6 AND DMSO-d_6/D_2O

Residue	DMSO-d_6	DMSO-d_6/D_2O (40%)	$\Delta\delta$ [a]
Pro CO	170.16	173.42	3.26
Tyr CO	170.65	173.00	2.35
Arg CO	173.28	173.52	0.24
Leu CO	170.85	171.11	0.26

Chemical shifts are given in ppm with respect to TMS.
[a] $\Delta\delta$ (ppm) is the difference in chemical shift between DMSO-d_6/D_2O (40%) and DMSO-d_6.

Proton spatial proximity was determined by using ROESY with a DANTE pulse train for solvent suppression [9]. A 5-mm inverse probe was used and the following experimental parameters were selected: SW was 4000 Hz in F2 and 2000 Hz in F1; incremented delay 3 μs; no. of increments 512; relaxation delay 2 s; matrix size (F1 × F2) 512×2K; acquisition time 0.57 s; number of scans 64; spin-locking time 250 ms. The spin-lock conditions were achieved using a series of hard pulses of small flip angle. Most ROESY experiments were free from spurious resonances due to magnetisation transfer between scalarly coupled spins, i.e. homonuclear Hartmann–Hahn transfer (HOHAHA) signals.

Fully decoupled ^{13}C NMR spectra were recorded with samples containing 25 mg (77 mM) of peptide on Bruker AM-360 and Nicolet QE-300 spectrometers. Attached proton test (APT), one-bond and long-range proton–carbon shift correlation spectra were obtained on the QE-300 apparatus. Carbonyl shifts and $^3J(COCH^\beta)$ were assigned by Dr. J. Richardson using a 500 MHz Bruker instrument at Cambridge University [10], employing proton-observed long-range heteronuclear shift correlation experiments and an interleaved TOCSY spectrum for obtaining reference multiplets. Experimental conditions involved acquisition of 800 t_1 increments with a ^{13}C spectral width of 33 000 Hz and a ^1H spectral width of 5000 Hz in F2.

Molecular modelling

All calculations were performed on a Personal Iris 4D-20 workstation hosted by an Iris 4D-280 Silicon Graphics computer, operating under the IRIX 4.01 operating system using the modelling program SYBYL, v. 6.0. Restrained molecular dynamics (RMD) and energy minimisations (EM) were performed using the Biopolymer dictionary method with charged N- and C-terminal groups to represent the natural charged state of the molecule. Molecular mechanics calculations were performed using a dielectric constant of 45 to represent DMSO, with Kollman all-atom types and charges. A BFGS minimiser was selected with the TAILOR option and structures were energy-minimised using MAXMIN2, yielding gradients with rmsd values of 0.01 kcal/mol prior to MD.

Restrained molecular dynamics simulations were performed with the DYNAMICS option in SYBYL. Intramolecular hydrogen bonds were constrained by applying a distance constraint between nominated NH and CO groups of 1.8–2.3 Å with a soft force constant of 5 kcal/mol. This was still strong enough to maintain the constraint during the entire RMD simulation. The following typical conditions were used for RMD using the SETUP option: coupling factor 10 fs; interval length 200 ps; write data every 100 fs; time step 1.0 fs; Boltzmann starting velocities random no; temperature 800 K.

Using the Sybyl Programming Language, a macro was employed to select the unique minima from the configurations produced from the RMD history file. The macro selects 400 of the lowest energy conformations, anneals them by dynamics at 300 K followed by MAXIMIN2 minimisation, and selects unique minima by the following criteria: energy difference < 0.1 kcal/mol, RMS_MATCH of backbone atoms < 0.3 Å and excluded volume < 3 Å [3]. The NMR data were compared with the computed structures by using the TABLE option for tabulating distances and torsions of interest.

Results and Discussion

NMR studies of proctolin

The ^1H NMR spectra of proctolin were studied in three different solvent systems; H_2O/D_2O, DMSO-d_6 and CD_3OH. Assignments were made by using double-quantum-filtered correlated spectroscopy (DQF-COSY) and homonuclear decoupling experiments. In Fig. 1 the ^1H NMR spectrum in DMSO-d_6 is shown. Many of the ^1H chemical shifts are shifted from their random coil values [11], suggesting a degree of structural preference. The largest differences from random coil are evident in DMSO-d_6. These differences may result from conformational effects and other factors, such as nearby aromatic rings and titratable groups. In Fig. 1 a minor species (~7.5%) with a *cis*-Pro conformation can be seen.

TABLE 3
OBSERVED NOEs FOR PROCTOLIN IN DMSO-d_6 AT 20 °C AND IN CD_3OH AT −30 °C

NOE no.	NOE	Solvent	
		DMSO-d_6	CD_3OH
1	Tyr NH···Arg CH^α	w[a]	none
2	Tyr CH^α···Tyr CH(ortho)	s	w
3	Tyr CH^α···Leu NH	s	w
4	Leu NH···Leu CH_2^β	w	s
5	Leu CH^α···Leu Me	s	s
6	Leu CH^α···Pro CH_2^δ	s	s
7	Pro CH^α···Thr NH	s	s
8	Thr NH···Thr Me	w	none

[a] Qualitative evaluation of the strength of the NOE based on the comparison with cross peaks involving the two geminal Tyr CH_2^β protons: s = strong NOE; w = weak NOE; none = no observable NOE.

TABLE 4
LOWEST ENERGIES FROM RESTRAINED MOLECULAR DYNAMICS SIMULATIONS AFTER ANNEALING AND ENERGY MINIMISATION FOR THE VARIOUS TURN STRUCTURES OF PROCTOLIN[a]

Turn		Energy (kcal/mol)
(i) α-turn	Arg C=O···NH Thr	11.33
(ii) β-turn	Tyr C=O···HN Thr	9.33
(iii) γ-turn	Leu C=O···HN Thr	9.16
(iv) –	No restraint	9.69

[a] For the RMD and energy minimisation a dielectric constant of 45 was used to simulate DMSO-d_6.

Hydrogen bonding

Intramolecular hydrogen bonds are useful determinants of secondary structure in small peptides, because they act as markers for defining turns [12]. Temperature coefficients of NH chemical shifts ($\Delta\delta_{NH}$ / T ($\times 10^{-3}$) ppm/°C) were used to identify hydrogen-bonded NHs as shown in Table 1. The particularly low value for Thr NH (1.20×10^{-3} ppm/°C) in DMSO-d_6 suggests its involvement in an intramolecular hydrogen bond. The Thr NH temperature coefficient increases with the proton-donating power of the solvent, suggesting the hydrogen bond is weakened by competing intermolecular hydrogen bonding of the solvent. The high temperature coefficient for Leu NH indicates its accessibility to solvent compared to the other NHs.

The results suggest that Thr NH is involved in an intramolecular hydrogen bond in DMSO-d_6, but they do not indicate to which proton acceptor group it is bound. Hydrogen-bonded carbonyl groups can be identified [13] by monitoring changes in the carbonyl carbon chemical shifts upon titrating solutions of the peptide in DMSO-d_6 with D_2O. The intramolecular hydrogen-bonded carbonyl carbons exhibit little change in chemical shift upon diluting DMSO-d_6 with a proton (deuteron) donor solvent (D_2O), in contrast to carbonyl resonances that are not hydrogen bonded and are shifted downfield by 2–3 ppm. The chemical shifts of the four peptide carbonyls are listed in Table 2 for DMSO-d_6 and DMSO-d_6/D_2O (40%). As shown, the Pro CO and Tyr CO resonances are shifted downfield by 2–3 ppm, but the Arg CO and Leu CO are shifted by only 0.24 and 0.26 ppm, respectively. This suggests that either Arg CO or Leu CO is hydrogen-bonded to the Thr NH: the former results in an α-turn, 1→5 hydrogen bond, and the latter in a γ-turn, 3→5 hydrogen bond. We consider it unlikely that both carbonyls are hydrogen-bonded to Thr NH, due to the strained internal geometry of this conformation.

NOEs and low-temperature studies

Aqueous solutions of proctolin exhibit little evidence of secondary structure. The high viscosity of DMSO-d_6 and its proton-acceptor ability appear to limit the conformational freedom of proctolin. NOEs were measured both in DMSO-d_6 at 20 °C and in CD_3OH at −30 °C, and are listed in Table 3. The observed NOEs are mainly related to four amino acids and provide distance constraints for the sequence Thr-Pro-Leu-Tyr. Most of the NOEs are short-range and involve interresidue NH···CH^{α} NOEs (e.g. NOEs 1, 3 and 7) and intraresidue backbone–side-chain NOEs (e.g. NOEs 2, 4, 5 and 8). The only exception is the NOE that defines the *trans*-Pro (i.e. NOE 6). The weak NOE associated with arginine (Arg CH^{α}···Tyr NH) suggests that this residue is conformationally mobile in solution. The lack of long-range NOEs suggests that if any turn is present, it is likely to be a small γ-turn. The NMR data are most consistent with a γ-turn between Thr NH and Leu CO.

Molecular modelling studies of proctolin

A modelling strategy for proctolin was sought that could consolidate the NMR observations [14]. The NMR studies indicate that there is at least one (or more) conformational state. We considered two different ap-

TABLE 5
COMPARISON BETWEEN EXPERIMENTAL NOEs AND PREDICTIONS FROM RESTRAINED MOLECULAR DYNAMICS FOR PROCTOLIN

NOE no.	NOE	Experimental strength[a]	Predicted strength of NOE[b]			
			α-turn	β-turn	γ-turn (inverse)	No restraint
1	Tyr NH···Arg CH^{α}	w	w	s	w	s
2	Tyr CH^{α}···Tyr CH(ortho)	s	s	s	s	w
3	Tyr CH^{α}···Leu NH	s	w	s	s	s
4	Leu NH···Leu CH_2^{β}	w	w	s	w	w
5	Leu CH^{α}···Leu Me	s	w	w	w	w
6	Leu CH^{α}···Pro CH_2^{δ}	s	w	w	s	s
7	Pro CH^{α}···Thr NH	s	w	w	s	w
8	Thr NH···Thr Me	w	w	w	w	w
	No. of NOEs consistent in strength between experimental and predicted		4	3	7	4

[a] In DMSO-d_6, as given in Table 3.
[b] w = weak NOE, corresponding to a calculated distance of 2.50–4.0 Å; s = strong NOE, corresponding to a calculated distance of 1.85–2.50 Å.

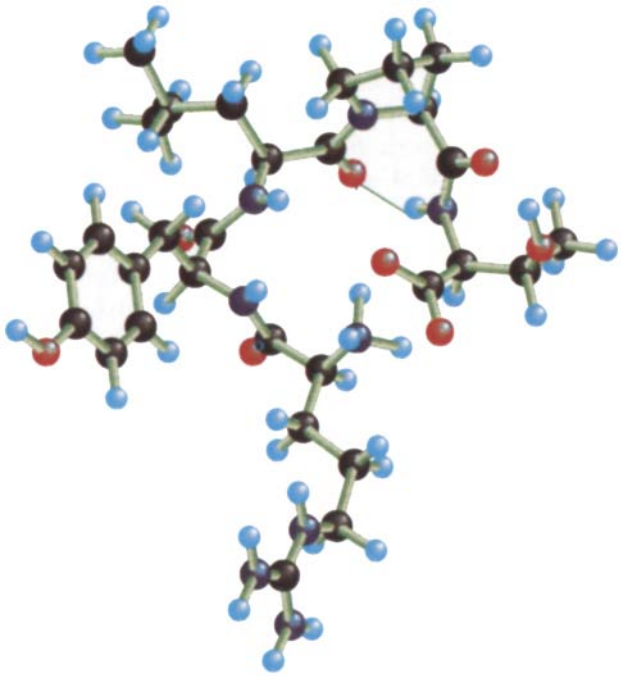

Fig. 4. γ-Turn for proctolin, showing a hydrogen bond between Thr NH and Leu CO.

proaches for tackling this problem: (i) 'best-fit' and (ii) molecular construction [15].

We finally used the 'best-fit' approach for modelling proctolin, focusing on generating low-energy conformers that would be consistent with the DMSO-d_6 NMR data. The NMR data suggest that Thr NH is hydrogen-bonded either to Leu CO or to Arg CO. Modelling was used to identify the most probable hydrogen-bonded carbonyl. The following three models of the peptide, containing C=O···HN hydrogen bonds, were constructed:

(i) α-turn Arg C=O···HN Thr
(ii) β-turn Tyr C=O···HN Thr
(iii) γ-turn Leu C=O···HN Thr

A distance constraint was used to represent the hydrogen bond in three separate ((i)–(iii)) restrained molecular dynamics simulations. A fourth simulation (iv) had no constraints and this one was used as a control, and to see whether the molecule shows a predisposition for formation of a particular turn.

The minimum energies for all simulations are listed in Table 4. Of the four simulations, the γ-turn results in the lowest energy, but the differences in energy between the various turn types are sufficiently small to render significant population of conformations other than just the γ-turn a strong possibility.

Simulations of NOEs

The NOEs were classified into two main classes: (i) strong (distance = 1.85–2.50 Å); and (ii) weak (distance = 2.50–4.0 Å). These classes were based on the peak intensities in the ROESY spectrum, as shown in Fig. 2. The NOEs according to this classification are listed in Table 5, while calculated NOEs based on distances in typical simulations are shown in Fig. 3. As shown in Table 5, all experimentally observed NOEs are feasible for each of the calculated turns. However, their relative ranking (weak versus strong) is different. The turn that is most consistent with the NOEs is the γ-turn. In the simulation without any constraint, (iv), a tendency to form a γ-turn was observed as well. This was evident for a number of low-energy structures containing a hydrogen bond between Thr NH and Leu CO. No disposition for formation of other hydrogen bonds was observed.

Spectroscopic and modelling studies of proctolin analogues

N-methylated and C-methylated derivatives of proctolin were synthesised with the aim of producing proctolinergic peptides with enhanced protease stability. We prepared *N*-methyl-Tyr and C^{α}-methyl-Tyr derivatives, because in vivo proteolysis is believed to occur at the tyrosine residue. The *N*-methyl-Leu analogue was also synthesised to stop possible proteolysis of the Leu-Tyr amide bond. The conformational consequences of these chemical modifications were assessed by ^{1}H NMR spectrosocopy and molecular modelling, with the aim of identifying secondary structure and postulating qualitative structure–activity relationships.

N-methyl-Leu-proctolin The NH temperature coefficients (Δδ/T) of *N*-methyl-Leu-proctolin, as shown in Table 6, follow a similar trend as for proctolin. The Thr NH coefficient is larger, which indicates either a weaker

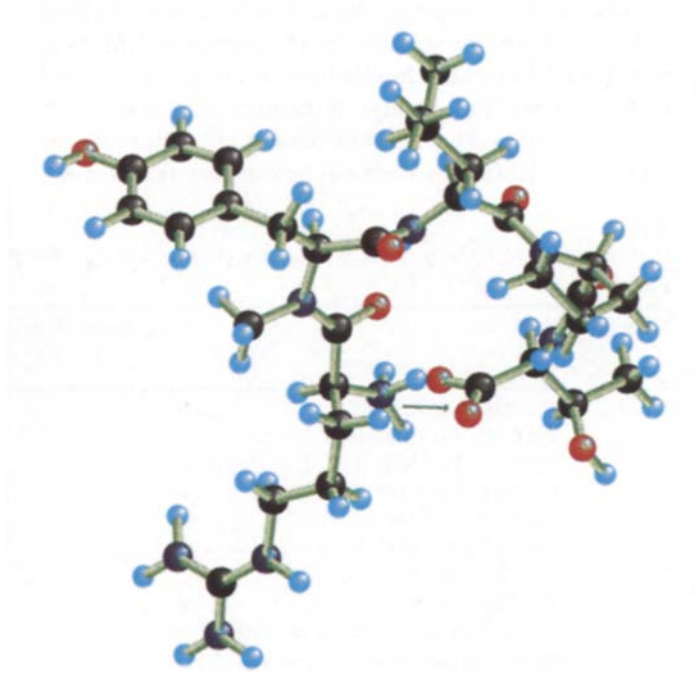

Fig. 5. Model, generated by molecular dynamics, for the salt bridge in the *N*-methyl-Tyr-proctolin analogue.

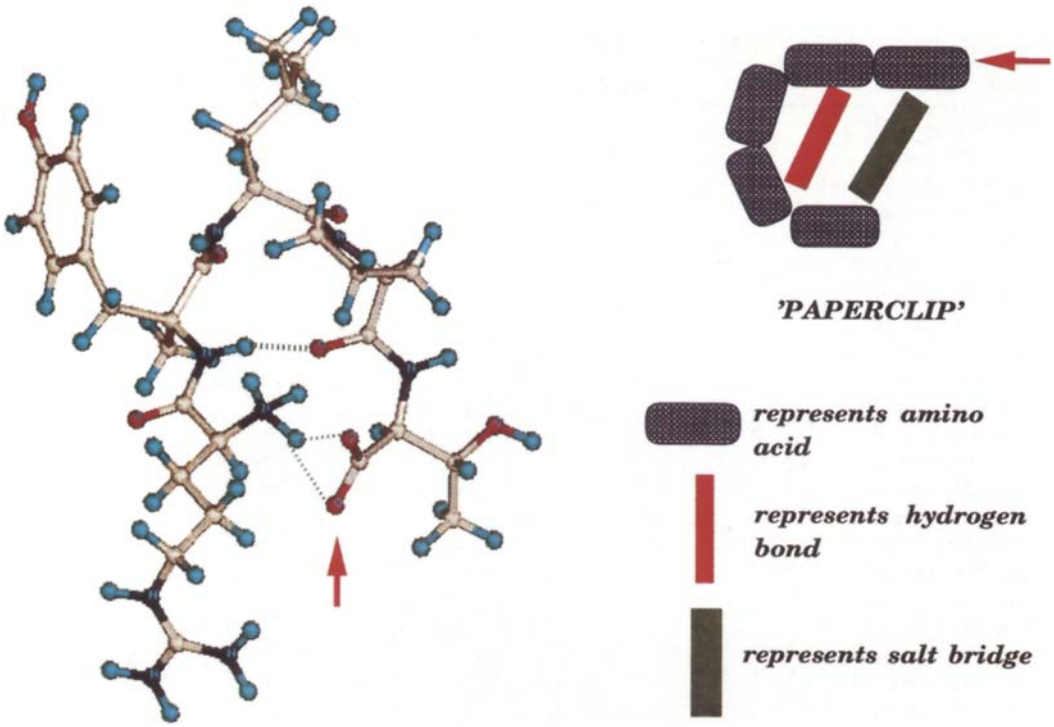

Fig. 6. 'Paperclip' molecular dynamics model for C^{α}-methyl-Tyr-proctolin.

hydrogen bond or a smaller concentration of the hydrogen-bonded form. The solution contained ca. 10.7% *cis*-proline conformer.

The NOEs were similar to those of proctolin, as shown in Table 7. The results suggest that N-methylation of leucine produces a compound with a similar secondary structure as proctolin, but a weaker hydrogen bond between Thr NH and Leu CO.

N-methyl-Tyr-proctolin The NH and CH^{α} proton chemical shifts of *N*-methyl-Tyr-proctolin are significantly different from those of proctolin. Literature values for NH_3^+ temperature dependencies in peptides have not been reported, but the small temperature coefficient for Arg NH_3^+ in this analogue suggests its involvement in a salt bridge with the terminal carboxylate of Thr. There is no other indication for intramolecular hydrogen bonding.

In addition to the NOEs observed for proctolin, there are also three strong NOEs involving Leu $CH^{\alpha}\cdots$Tyr CH^{α} (NOE 11), Leu $NH\cdots$Pro CH_2^{δ} (NOE 12), and Thr $NH\cdots$Pro CH_2^{β} (NOE 17). NOEs between $CH^{\alpha}\cdots CH^{\alpha}$ protons are usually associated with cis-amide bonds. A cis-amide bond for Leu seems unlikely because this amino acid is not N-methylated. Molecular models of *N*-methyl-Tyr-proctolin that are constrained by the observed NOE distances turn out to be consistent with a salt bridge between the terminal Arg NH_3^+ and Thr CO_2^-, as shown in Fig. 4. The remaining amidic NHs, Leu NH and Thr NH, are oriented outwards to the surrounding solvent and exhibit high temperature coefficients.

C^{α}-methyl-Tyr-proctolin In contrast to proctolin, in the ^1H NMR spectrum of C^{α}-methyl-Tyr-proctolin all OHs were resolved. A downfield signal at 12.5 ppm, not

TABLE 6
NMR AMIDE PROTON TEMPERATURE COEFFICIENTS FOR PROCTOLIN AND ANALOGUES IN DMSO-d_6 [a]

Peptide[b]	$\Delta\delta/T$ ($\times 10^{-3}$; ppm/°C)[c]					
	Arg NH_3^+	Arg NH	Arg NH_2	Tyr NH	Leu NH	Thr NH
Proctolin	5.06		5.06	4.67	8.67	1.20
N-Me-Leu-	[d]	[d]	4.70	5.00	–	2.99
N-Me-Tyr-	0.85	3.50	[d]	[d]	6.50	5.90
C^{α}-Me-Tyr-	1.50	3.00	2.59	1.79	6.20	6.52
Cycloproctolin	4.84 (NH)	2.22	[d]	1.04	4.74	3.18

[a] Temperature range: 30–60 °C at 5 ° intervals.
[b] Proctolin or proctolin derivative.
[c] Coefficient of change in chemical shift with temperature.
[d] NH peaks broadened due to exchange with residual water.

TABLE 7
OBSERVED NOEs FOR PROCTOLIN AND ITS ANALOGUES IN DMSO-d_6 [a]

NOE no.	NOE	Proctolin	*N*-Me-Leu-	*N*-Me-Tyr-	C^{α}-Me-Tyr-
1	Tyr NH···Arg CH^{α}	w	w	–	s
2	Tyr CH^{α}···Tyr 2,6	s	s	s	–
3	Tyr CH^{α}···Leu NH	s	–	s	–
4	Leu NH···Leu CH_2^{β}	w	–	w	s
5	Leu CH^{α}···Leu Me	s	s	s	s
6	Leu CH^{α}···Pro CH_2^{δ}	s	s	s	s
7	Pro CH^{α}···Thr NH	s	s	s	s
8	Thr NH···Thr Me	w	w	w	w
9	Leu CH^{α}···Leu NMe	–	s	–	–
10	Leu NMe···Tyr 2,6	–	s	–	–
11	Leu CH^{α}···Tyr CH^{α}	–	–	s	–
12	Leu NH···Pro CH_2^{δ}	–	–	s	–
13	Tyr CH^{α}···Tyr 3,5	–	–	w	–
14	Tyr NMe···Arg CH^{α}	–	–	s	–
15	Arg NH_3^+···Arg CH_2^-	–	–	w	w
16	Thr CH^{α}···Pro CH^{α}	–	–	w	–
17	Thr NH···Pro CH_2^{β}	–	–	s	–
18	Leu CH^{α}···Tyr 2,6	–	–	–	w
19	Leu CH^{α}···Tyr 3,5	–	–	–	w
20	Arg CH_2^{β}···Tyr NH	–	–	–	w
21	Leu NH···Tyr C^{α}Me	–	–	–	s
22	Leu NH···Tyr 2,6	–	–	–	w
23	Arg CH_2^{β}···Tyr 2,6	–	–	–	w
24	Arg CH_2^{β}···Arg NH	–	–	–	w

[a] Qualitative evaluation of the strength of the NOE based on the comparison with cross peaks involving the two geminal Tyr CH_2^{β} protons: s = strong NOE; w = weak NOE; – = no observable NOE.

present in the spectra of the other analogues, was attributed to CO_2H, which may be involved in intramolecular hydrogen bond formation (i.e. $CO_2^-\cdots{}^+H$) [16]. The small temperature dependence of the Tyr NH shift (Table 6) indicates its involvement in an intramolecular hydrogen bond with one of the backbone carbonyl oxygen atoms, either Thr CO_2^- or Pro CO. This is unusual, because it would implicate a hydrogen-bonding arrangement extending from the C-terminal end, rather than from the N-terminal end. The low temperature coefficient of Arg

TABLE 8
COMPARISON BETWEEN OBSERVED NOEs AND PREDICTIONS FROM RESTRAINED MOLECULAR DYNAMICS FOR C^{α}-methyl-Tyr-PROCTOLIN

NOE no.	NOE	Experimental strength[a]	Predicted strength of NOE[b] for particular model		
			Tyr NH···Thr CO_2 [c]	Tyr NH···Pro CO [c]	No restraint
1	Tyr NH···Arg CH^{α}	s	s	s	s
4	Leu NH···Leu CH_2^{β}	s	s	s	s
5	Leu CH^{α}···Leu Me	s	s	s	s
6	Leu CH^{α}···Pro CH_2	s	w	w	s
7	Pro CH^{α}···Thr NH	s	–	s	s
8	Thr NH···Thr Me	w	w	w	w
16	Arg NH_3^+···Arg CH_2^{δ}	w	s	s	s
19	Leu CH^{α}···Tyr 2,6	w	w	w	w
20	Leu CH^{α}···Tyr 3,5	w[d]	–	–	–
21	Arg CH_2^{β}···Tyr NH	w	s	s	s
22	Leu NH···Tyr C^{α}Me	s	w	w	w
23	Leu NH···Tyr 2,6	w	s	s	w
24	Arg CH_2^{β}···Tyr 2,6	w	w	w	w
25	Arg CH_2^{β}···Arg NH	w	s	s	s

[a] In DMSO-d_6, as given in Table 7.
[b] w = weak NOE, corresponding to a calculated distance of 2.50–4.0 Å; s = strong NOE, corresponding to a calculated distance of 1.85–2.50 Å; – = no NOE expected; calculated distance > 5.0 Å.
[c] Hydrogen bond treated as a constraint in RMD.
[d] Negative cross peak, arising from HOHAHA-transfer pathway.

TABLE 9
COMPARISON OF OBSERVED CYCLOPROCTOLIN NOEs AND PREDICTIONS USING RESTRAINED MOLECULAR DYNAMICS

NOE no.	NOE	Experimental strength[a]		Predicted strength of NOE[b]
		Proctolin	Cycloproctolin	
1	Tyr NH···Arg CH^{α}	w	none	
2	Tyr CH^{α}···Tyr 2,6	s	s	s
3	Tyr CH^{α}···Leu NH	s	s	s
4	Leu NH···Leu CH_2^{β}	w	s	s
5	Leu CH^{α}···Leu Me	s	s	s
6	Leu CH^{α}···Pro CH_2^{δ}	s	none	-
7	Pro CH^{α}···Thr NH	s	s	s
8	Thr NH···Thr Me	w	w	w
16	Arg NH^{α}···Arg CH_2^{δ}	none	w	w
18	Thr NH···Pro CH_2^{β}	none	w	w
26	Leu NH···Tyr NH	none	s	s
27	Leu NH···Thr CH^{α}	none	s	w
28	Thr NH···Thr CH^{β}	none	s	s
29	Arg NH^{α}···Tyr CH^{α}	none	s	s
30	Arg NH^{α}···Tyr NH	none	w	w
31	Arg CH^{α}···Tyr 2,6	none	w	w
32	Leu CH^{α}···Pro CH^{α}	none	s	s
33	Thr NH···Leu CH^{α}	none	s	w
34	Arg NH^{α}···Arg CH^{δ}	none	w	w
35	Tyr 3,5···Pro CH^{δ}	none	w	w
36	Tyr NH···Leu CH^{α}	none	w	w

[a] In DMSO-d_6.
[b] w = weak NOE, corresponding to a calculated distance of 2.50–4.0 Å; s = strong NOE, corresponding to a calculated distance of 1.85–2.50 Å; none = no NOE observed; – = no NOE expected; calculated distance > 5.0 Å.

NH_3^+ may also suggest the presence of a salt bridge between the terminal Arg NH_3^+ and the terminal carboxyl.

The NOEs shown in Table 7 suggest a different and more compact secondary structure compared to proctolin. Many more NOEs are observed, some of which are long-range. Molecular models for (i) and (ii) were constrained as follows:

(i) Comprises an intramolecular hydrogen bond between Tyr NH and Thr CO_2^-:

Arg-Tyr-Leu-Pro-Thr
4 3 2 1
NH·····^-O_2C

(ii) Comprises an intramolecular hydrogen bond between Tyr NH and Pro CO:

Arg-Tyr-Leu-Pro-Thr
4 3 2 1
NH·····OC

The molecular dynamics simulations did not fully reproduce all experimental data, as shown in Table 8. The lowest energy conformers were obtained with model (ii), forming a so-called 'paperclip' conformation [17,18], because of the resemblance in shape if viewed along the helix axis (Fig. 5).

We conclude that C^{α}-methyl-Tyr-proctolin is present in DMSO-d_6 as a 'paperclip', stabilised by an intramolecular hydrogen bond between Tyr NH and Pro CO and possibly by a salt bridge between Arg NH_3^+ and Thr CO_2^-.

Spectroscopic and modelling studies of cycloproctolin

Rigidity was introduced into proctolin by linking the N- and C-terminal groups, resulting in an amide bond. The ^1H chemical shift data for cycloproctolin are significantly different from those of proctolin, suggesting a different secondary structure. As for C^{α}-methyl-Tyr-proctolin, the temperature dependences of the NH chemical shifts (see Table 6) suggest that Tyr NH ($\Delta\delta/T = 1.04 \times 10^{-3}$ ppm/K) takes part in an intramolecular hydrogen bond. The only two candidate carbonyl oxygen acceptors for this hydrogen bond are Thr CO and Pro CO.

Table 9 shows that there are several NOEs observed in the ROESY spectrum of cycloproctolin that are not observed in proctolin or the other analogues. One of these NOEs (no. 32) is a strong one between Pro CH^{α} and Leu CH^{α}, which indicates a *cis*-amide-proline bond.

Dynamics simulations performed without constraints indicate that there is a large tendency for formation of the intramolecular hydrogen bond Tyr NH···O=C Thr. In these simulations both the experimentally observed preference for a *cis*-amide proline and the observed NOEs could be reproduced. The only peptide structural motif consistent with these data is a β-bulge loop [17] (see Fig. 6), which comprises a bifurcated intramolecular hydrogen bond from Tyr NH to Thr CO and Pro CO. It is import-

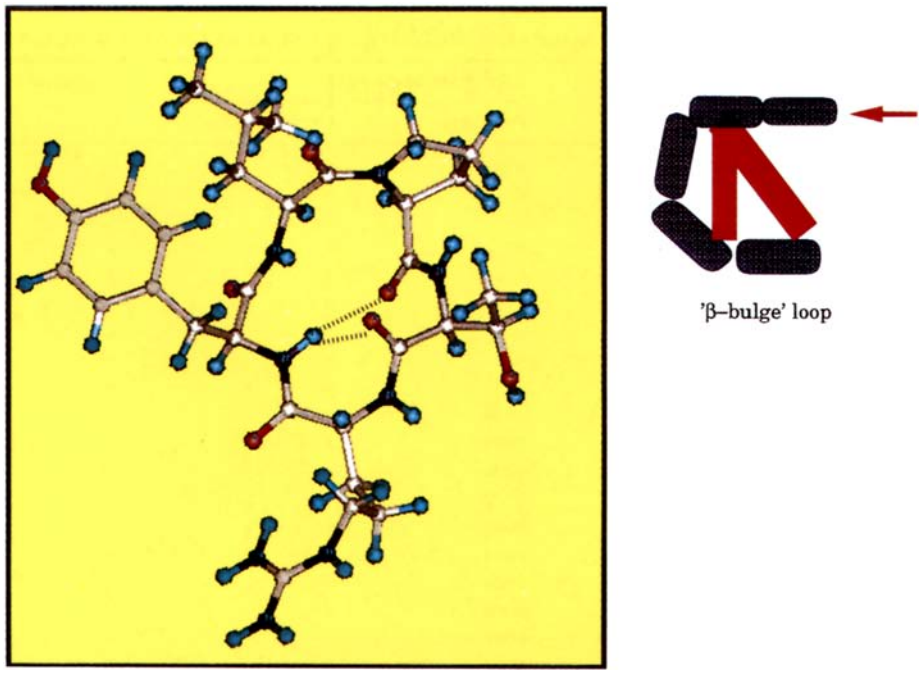

Fig. 7. Molecular dynamics model for cycloproctolin, showing a 'β-bulge' loop with a hydrogen bond between Tyr NH and Pro CO and Thr CO.

ant to note that there is a spatial similarity between this loop and the 'paperclip' loop found for C^{α}-methyl-Tyr-proctolin.

Structure–activity studies

The kinetic data for the five pentapeptides in Table 10 were derived from their myotropic properties, as measured by the extent of contraction in the foregut tissue of desert locusts. Their efficacies were estimated from the effect of maximum contraction elicited by proctolin in the absence of an antagonist.

The antagonists C^{α}-methyl-Tyr-proctolin and cycloproctolin were distinguished from agonists by being unable to cause tissue contraction, but they were able to reduce the contractile effects of proctolin. The effects of antagonists on the efficacy, ED_{25}, and latency values for

TABLE 10
MYOTROPIC ACTIVITIES OF PROCTOLIN AND ITS ANALOGUES FROM DOSE–RESPONSE CURVES ON THE FOREGUT OF DESERT LOCUSTS

Peptide and concentration (M) to elicit response	Activity	Efficacy[a]	ED_{25} (10^{-8} M) [b]	Latency[c]	Structure[d]
Proctolin	Full agonist	1.00	8.0	0 ± 4.8	Inverse γ-turn Thr NH···Leu CO
N-Me-Tyr-proctolin	No effect				Possible salt bridge
1×10^{-6}		0.88	12	2.8 ± 3.6	Arg NH_3^+-Thr CO_2^-
1×10^{-5}		1.03	8.0	4.0 ± 4.4	
C^{α}-Me-Tyr-proctolin	Strong antagonist				'Paperclip' loop
1×10^{-8}		0.55	33	12.4 ± 4.4	Tyr NH···Pro CO
1×10^{-7}		0.27	160	22.8 ± 5.6	
1×10^{-6}		0.12	–	34.0 ± 8	
Cycloproctolin	Medium antagonist				β-Bulge loop
5×10^{-7}		1.02	13	4.4 ± 6.4	Tyr NH···Thr CO,
1×10^{-6}		0.70	20	6.0 ± 5	Pro CO
5×10^{-6}		0.63	20	19.6 ± 8.4	
N-Methyl-Leu-proctolin	Partial agonist	0.52	4500	19.6 ± 3.6	Weak inverse γ-turn Thr NH···Leu CO

[a] Efficacy = maximum effect of contraction elicited by proctolin in the presence of the antagonist.
[b] ED_{25} = concentration of proctolin required to elicit 25% of the maximum contraction induced by 10^{-6} M proctolin on desert locust foregut.
[c] Latency = onset of a response to peptide injection; this is a measure of the length of time taken for an antagonist or agonist to bind to the receptor.
[d] Structure = favoured conformation on the basis of NMR and modelling.

proctolin give an indication of the strength of binding and the binding location (e.g., the same site or allosteric binding site as proctolin). Although the data set is too small to reach firm conclusions at this stage, the results shown in Table 10 do suggest that there are different and highly specific secondary structural requirements for agonist and antagonist activity. Small alterations in the backbone atoms appear to have a definite effect on both structure and activity. Thus agonists may require a more open structure, involving the location of an inverse γ-turn between Thr NH and Leu CO higher up in the sequence, whereas antagonists require a more compact structure, involving a loop rather than a turn between Tyr NH and Pro CO lower down in the sequence, possibly stabilised by a salt bridge between N- and C-terminal groups.

Conclusions

The only element of secondary structure for proctolin that has been identified in these studies is found in DMSO-d_6. In this solvent the predominant conformation of the peptide is extended at the N-terminal end of the sequence, but constrained to form an inverse γ-turn with an intramolecular hydrogen bond between residue 5 (Thr NH) and residue 3 (Leu CO). The inverse γ-turn is destabilised in protic solvents, such as methanol and water.

N-methylation and C^{α}-methylation were explored as ways of protecting proctolin against metabolic proteolysis. Cyclisation was also examined as a method of introducing rigidity into the molecule, without destroying functionality. These modifications had marked effects on both biological activity and secondary structure.

Synthetic targets based on the antagonist C^{α}-methyl-Tyr-proctolin may be more attractive than those based on proctolin, since the 'paperclip' loop structure of the former has greater rigidity. The structure of cycloproctolin in solution is similar to that of C^{α}-methyl-Tyr-proctolin and the compound also shows antagonist activity. Such observations may provide insight into the design of proctolinergic-acting compounds.

Further studies are required for a more comprehensive understanding of the conformations of proctolin in the unbound state and in receptor–ligand complexes, although the latter must await isolation of proctolin receptors.

Acknowledgements

The authors would like to thank the following people for useful comments and contributions: Dr. M. Anderson, Dr. P. Regan, Mrs. S. Potter, Dr. D. Neuhaus, Dr. A.S. Gray, Dr. J. Bearder, Mr. P. Jewess, and Dr. J. Richardson.

References

1 Brown, B.E. and Starratt, A.N., J. Insect Physiol., 21 (1975) 1879.
2 Holman, G.M. and Hook, B.J., Agricultural Research Service Workshop on Insect Neuropeptides, Insect Peptides and Bioregulation, College Station, TX, U.S.A., June 1982, Southwest Entomol., Suppl. 0(5), (1983) 24.
3 Lange, A.B., Orchard, I. and Konopinska, D., J. Insect Physiol., 39 (1993) 347.
4 Osborne, R.H., Banner, S.E. and Wood, S.J., Comp. Biochem. Physiol. C Comp. Pharmacol. Toxicol., 96 (1990) 1.
5 Gray, A.S., Osborne, R.H. and Jewess, P.J., J. Insect Physiol., 40 (1994) 595.
6 Lange, A.B., Orchard, I. and Belanger, J.H., J. Neurobiol., 20 (1989) 470.
7 Orchard, I. and Belanger, J.H., J. Exp. Biol., 174 (1993) 321.
8 Williamson, M.P. and Waltho, J.P., Chem. Soc. Rev., (1992) 227.
9 Rabenstein, D. and Larive, C.K., J. Magn. Reson., 87 (1990) 352.
10 Richardson, J., Ph.D. Thesis, University of Cambridge, Cambridge, U.K., 1993.
11 Wüthrich, K., NMR of Proteins and Nucleic Acids, Wiley, New York, NY, 1986.
12 Jardetzky, O. and Roberts, G.C.K., NMR in Molecular Biology, Academic Press, London, U.K., 1981.
13 Urry, D.W., Mitchell, L.W. and Ohnishi, T., Proc. Natl. Acad. Sci. USA, 71 (1974) 3265.
14 Neuhaus, D. and Williamson, M.P., The Nuclear Overhauser Effect in Structural and Conformational Analysis, VCH Publishers, New York, NY, 1989.
15 Landis, C. and Allured, V.S., J. Am. Chem. Soc., 113 (1991) 9493.
16 Hruby, V.J., Life Sci., 31 (1982) 189.
17 Milner-White, E.J., Biochem. Soc. Trans., 15 (1987) 506.
18 Milner-White, E.J., Trends Biochem. Sci., 12 (1987) 189.